Drilling for Polygons

Barry Cox and Stan Wagon

Abstract. We solve the problem of designing a simple device that uses rotary motion to drill a hole with a cross-section that is a regular polygon with an odd number of sides: the main idea is to use a polygonal trammel and a family of rotors. By using different rotors, one can produce a hole with a cross-section that is in any proportion of the trammel size from zero to exactly one. The key geometric idea is a result about the envelope of the edge of a triangle that rotates so that the other two edges maintain tangential contact with two fixed circles.

1. INTRODUCTION. The problem of drilling a hole with noncircular cross-section is one of long-standing engineering interest. In 1914 James Watts had the idea of rotating a Reuleaux triangle within a square; that was the basis of a tool that produced holes with an almost-square cross-section. Figure 1 shows the region (gray) that would be cut out by such a rotor. His idea was so successful that it was the foundation of the Watts Brothers Tool Works in Wilmerding, Pennsylvania, still in operation today (see [**G**] for an image of the Watts device). When the Reuleaux triangle rotates smoothly within a square housing (clockwise in Fig. 1), the three cutting bits trace out a curve that is almost, but not exactly, a square. Thus while the device has practical value, it is not a mathematically precise solution to the square-drill problem.

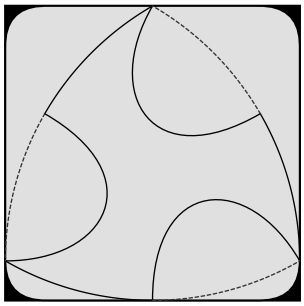

Figure 1. A drill bit that cuts an almost-square hole.

The problem of producing a perfect square was solved in 1939 by a contributor to *Mechanical World*. The anonymous author modified the Reuleaux triangle idea, using instead a shape bounded by four circular arcs and placing the cutting bit at the center of the non-Reuleaux arc, point C in Figure 2. This construction produces a mathematically exact square and also has the desirable property that the cutting tool at C comes to a stop each time the point passes through a corner. This construction was described by Bryant and Sangwin [**BS**, §10.4, Plate 21], who also describe a physical device they produced based on this construction which works quite well (see the animation at the URL cited in [**BS**]).

The location of the square-cutting point in the interior of the rotor means that one cannot make an open cutting edge as in the Watts case. Rather, one would attach a sharpened tool with the business end at C, as shown in black in Figure 2, right (see [**W**] for an animation of the motion). The white circle is the round hole that one would start with in practice; the square driller is then used at the next stage, to clean out the corners. Note that all such devices are meant to be driven by standard circular motion of one end, as in a drill press. To transform such motion to the combination of rotation and translation needed to keep the rotor inside its surrounding square, which we call a *trammel*, one uses the classic mechanism called an Oldham coupling; a 3-dimensional image of how this works is in [**CW**], with an animation at [**W1**].

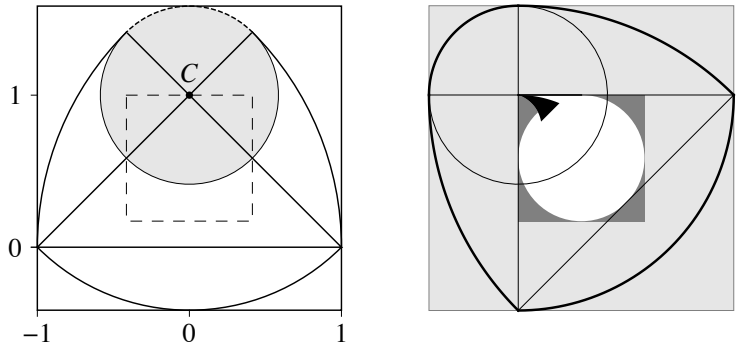

Figure 2. Point C traces out an exact square when the rotor is rotated inside the ambient square. The rotor is constructed by starting with the isosceles right triangle with vertex at C, forming the two circular arcs at left and right, adding the bottom arc centered at C, and then the upper arc, also centered at C. A cutting tool would be added at C in the shape shown at right, where the movement has progressed through 45° from the initial position.

In [**CW**] we extended the square-drill idea to show one to get an exact hexagonal hole (see animation at [**CW1**]). The extension was not entirely straightforward; a key technique for getting a proper rotor was the use of the envelope produced by rotating the trammel around part of the rotor. In [**CW**] we gave a full description of a hexagonal drill and indicated that an octagonal drill can likewise be constructed; we believe that all regular $2n$-gons can be handled using similar ideas, though it is not clear how to find a general proof. That paper concluded by posing the problem of drilling triangular holes, or holes in the shape of any regular polygon with an odd number of sides.

Here we describe a trammel-and-rotor device for which two points on the rotor trace out an exact regular n-gon where n is odd. In this construction the rotor may be any one of a family of rotors that work with a single trammel. Each rotor from the family will produce a polygonal locus that is a scaled-down copy of the polygon forming the trammel. The scaling ratio can be anything from 0 to 1. This feature might be of considerable practical importance in the physical manufacture of such a device, since a single trammel can be used with a set of rotors to produce variously sized polygonal holes. Another important practical point is that the speed of the cutting bit is 0 at the corners. The validity of our construction—by which is meant the fact that as the rotor rotates in the trammel it maintains sufficient contact with the sides so that its position is uniquely determined—relies on a certain inequality which we prove with the help of some computer algebra. One curiosity is that for a pentagonal hole the rotor turns out to be the intersection of two *fish bladders* (shapes known as *vesica pisces*).

The study of shapes (rotors) that rotate within polygons has a long history; see [**G1**] for a summary of several results. The surrounding polygon is often called the *stator*. These investigations typically require that the rotor touch all sides of the ambient polygon in every orientation. For the present work the key points are that the rotor touch sufficiently many sides so that it is stable and that it contain one or more points that trace out an exact regular n-gon. However, the case of the rotor for a triangle that we present in §4.1 does fit the criterion of earlier approaches, and was apparently first discovered by Reuleaux [**R**, chap. III].

2. A ROUND ENVELOPE. To find the curves that define the rotors we first solve an auxiliary problem: What is the envelope of the side of a triangle that rotates under the constraint that the other two sides maintain tangential contact with two fixed congruent circles (Fig. 3)? It turns out, serendipitously, that the envelope is simply a circular arc. We prove this by starting with a coordinate system so that the two circles of radius ρ are centered on the y-axis, symmetric in the x-axis, and with centers distance $2\,\delta$ from each other (Fig. 4). We then position ΔABC so that the envelope-generating side AB is vertical, with point D defined to be the intersection of AB with the horizontal line through C. The triangle is then defined in terms of the distance CD, denoted by η, and the angles $\angle DCA = \psi_1$ and $\angle BCD = \psi_2$; we'll use ψ for $\psi_1 + \psi_2$. Note that if angle $\angle A$ is obtuse, as it will be for some of our polygons, then D is outside AB and $\psi_1 < 0$. We now imagine rotating the triangle, letting θ be the angle of rotation: the angle between the rotated line CD and the x-axis. Because CD is perpendicular to BA we know that BA makes an angle of $\theta + \frac{\pi}{2}$ with the x-axis; and of course the axis's angle with CA (resp., CB) is $\theta + \psi_1$ (resp., $\theta - \psi_2$).

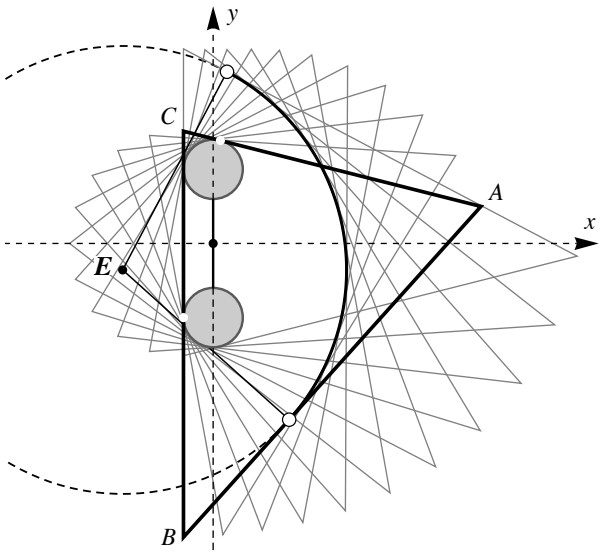

Figure 3. The envelope of a side of a triangle (AB) as the triangle rotates so that the other two sides touch two given circles is an arc of a circle.

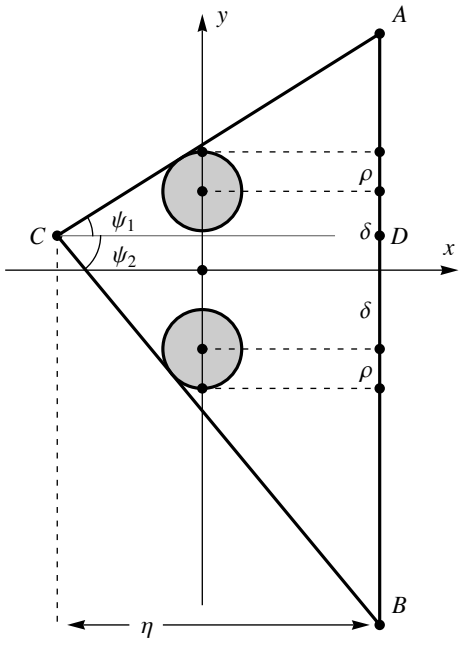

Figure 4. An envelope-defining triangle touching two congruent circles.

To ensure that CA remains in tangential contact with the upper circle, we require that line to pass through the point

$$(0, \delta) + \rho\left(\cos\left(\theta + \psi_1 + \frac{\pi}{2}\right), \sin\left(\theta + \psi_1 + \frac{\pi}{2}\right)\right) = (-\rho \sin(\theta + \psi_1), \delta + \rho \cos(\theta + \psi_1))$$

This means that the line CA is given parametrically in t_1 by $(0, \delta) + \rho\,(-\sin(\theta + \psi_1), \cos(\theta + \psi_1)) + t_1(\cos(\theta + \psi_1), \sin(\theta + \psi_1))$. Similarly CB must pass through $(\rho \sin(\theta - \psi_2), -\delta - \rho \cos(\theta - \psi_2))$ and is given by

$$(0, -\delta) + \rho\,(\sin(\theta - \psi_2), -\cos(\theta - \psi_2)) + t_2(\cos(\theta - \psi_2), \sin(\theta - \psi_2)).$$

Therefore C can be determined for an arbitrary orientation of the triangle by solving $CA = CB$ for t_1 and t_2, getting $t_1 = -(2\,\delta \cos(\theta - \psi_2) + \rho\,(1 + \cos\psi))\csc\psi$.

Using t_1 means that $C = (C_x, C_y)$ is given by

$$\begin{aligned} C_x &= -\left(2\,\delta \cos(\theta + \psi_1)\cos(\theta - \psi_2) + \rho\,(\cos(\theta + \psi_1) + \cos(\theta - \psi_2))\right)\csc\psi \\ C_y &= -\left(\delta \sin(2\,\theta + \psi_1 - \psi_2) + \rho\,(\sin(\theta + \psi_1) + \sin(\theta - \psi_2))\right)\csc\psi \end{aligned} \tag{1}$$

Because $D = (C_x + \eta\cos\theta, C_y + \eta\sin\theta)$, we can now express AB, which passes through D, in terms of a parameter t as $AB = (C_x + \eta\cos\theta - t\sin\theta, C_y + \eta\sin\theta + t\cos\theta)$.

Next we denote the parametric form of AB as (X, Y); then using (1) we get

$$\begin{aligned} X &= -\left(2\,\delta \cos(\theta + \psi_1)\cos(\theta - \psi_2) + \rho\,(\cos(\theta + \psi_1) + \cos(\theta - \psi_2))\right)\csc\psi + \eta\cos\theta - t\sin\theta \\ Y &= -\left(\delta \sin(2\,\theta + \psi_1 - \psi_2) + \rho\,(\sin(\theta + \psi_1) + \sin(\theta - \psi_2))\right)\csc\psi + \eta\sin\theta + t\cos\theta \end{aligned} \tag{2}$$

Finally, we can find the envelope of AB from the envelope equation: $\frac{\partial X}{\partial \theta}\frac{\partial Y}{\partial t} = \frac{\partial X}{\partial t}\frac{\partial Y}{\partial \theta}$ (a derivation of this is in [**CW**]). Solving gives $t = (2\,\delta \sin(\theta + \psi_1 - \psi_2) + \rho\,(\sin\psi_1 - \sin\psi_2))\csc\psi$, which can be substituted into (2) to get a parametric form of the envelope as $E + E_{\text{rad}}\,(\cos\theta, \sin\theta)$, where $E = (E_x, E_y)$ and the radius E_{rad} are given by

$$\begin{aligned} E_x &= -2\,\delta\,\cos\psi_1\cos\psi_2\csc\psi \qquad E_y = \delta\sin(\psi_1 - \psi_2)\csc\psi \\ E_{\text{rad}} &= \eta - \rho\,(\cos\psi_1 + \cos\psi_2)\csc\psi \end{aligned} \tag{3}$$

This proves that the envelope is a circle of radius E_{rad} centered at E.

Note that the θ that parametrizes the circle is the same θ that denotes the amount of rotation of the triangle; $\theta = 0$ means that the envelope-generating line is vertical. Note also that there is a natural start and finish to the rotation that yields the tangency: the starting position occurs when AC is vertical and the clockwise rotation concludes when BC is vertical. To be precise, and because we will use ϕ to parametrize the envelope arcs, this means that

$$\phi_{\min} = \psi_2 - \tfrac{\pi}{2} \text{ and } \phi_{\max} = \tfrac{\pi}{2} - \psi_1. \tag{4}$$

3. CONSTRUCTING AN ODD-GON DRILL. We now describe a construction that will produce a trammel and rotor that form a device to drill holes in the shape of an exact regular polygon with an odd number of sides. We will begin with a description for an arbitrary odd number of edges $n = 3, 5, 7, \ldots$ and then in §5.3 apply this method to give precise formulas for the case of triangular and pentagonal trammels. We use α to denote π / n.

We begin with a unit circle centered at the origin in a standard x-y coordinate system, in which we inscribe a regular n-gon, $n = 3, 5, 7, \ldots$, such that one vertex is at $(0, 1)$, with the opposite edge bisected by the negative y-axis at $y = -\cos\alpha$. This polygon is called the trammel and it has the form of a polygonal cavity in a plate or frame within which a rotor will rotate; we will assume the rotor rotates counterclockwise, with θ denoting the angle of counterclockwise rotation.

The objective in designing the rotor is to produce a curve that will have a fixed location in the trammel at all rotations and can smoothly move from one rotation to another; further, at least one point on the rotor should trace out an exact regular n-gon.

The rotor is constructed from $n - 1$ circular arcs, derived from the envelope results is §2, and two optional smaller circular arcs that will maintain constant contact with the trammel. They are optional because the radius of the smaller arcs, which we denote by r, satisfies $0 \le r \le \cos\alpha$ and for radius 0 these smaller arcs are absent. We start the construction with two circles of radius r centered on the y-axis at $y = 1 - r\sec\alpha$ and $y = r - \cos\alpha$. This will ensure that the upper circle starts with tangential contact with the two uppermost edges of the n-gon and the lower circle is in contact at the midpoint of the lowest n-gon edge. The central idea of the construction is that we imagine the rotor revolving inside the trammel with these two circles in constant direct contact with the trammel; therefore the center points of both circles will trace out an exact n-gon with outer radius $1 - r\sec\alpha$. The purpose of the remainder of the construction is to stabilize the location of the rotor in the trammel—meaning that for each orientation there is a unique position of the rotor—thus ensuring constant contact between the rotor's bounding circles and the trammel.

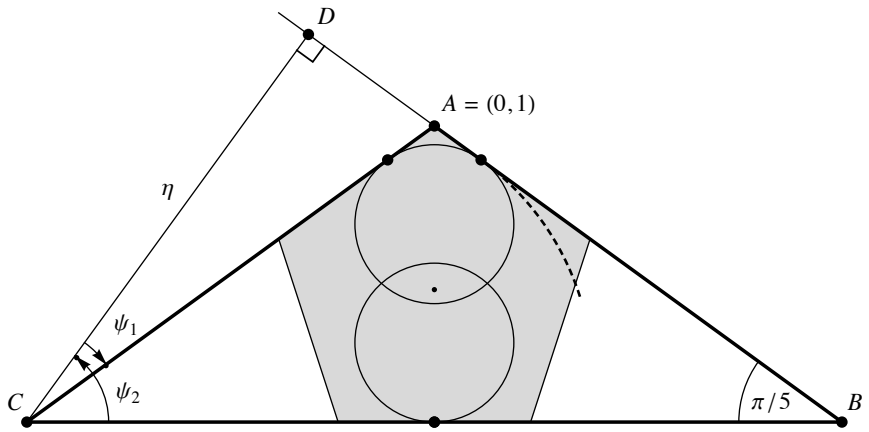

Figure 5. The circular envelope result of §2 can be applied to the triangle derived from two sides of a polygon to get the dashed envelope. Here $r = 3/5 \cos(\pi/5)$; note that $\psi_1 = \angle ACD$ is negative. The central point is $(0, 0)$, the center of the polygon; the two circles are symmetric about $y = y_0 = 0.038\ldots$.

Another way of considering the problem of designing the remainder of the rotor is to imagine the rotor is fixed and the trammel is rotating clockwise around the two circles with which we start the definition of the rotor. In this way we can determine the shape of the rotor as given by the parts of the envelopes of each edge of the polygon as it goes through this rotation.

One advantage of designing a rotor for a polygon with an odd number of edges is that the two edges in contact with the upper and lower circles are never parallel and therefore contact with any one of the edges on the right-hand side of the polygon will fix the rotor's position in the trammel. To be precise, if a shape S fits inside a polygon with three points of contact as indicated by the dots in Figure 5 (i.e., touching a side of the polygon on either side of a vertex and also the side opposite that vertex), then there is no nonzero vector $\boldsymbol{v}$ such that $S + \boldsymbol{v}$ is inside the polygon. Here is a formal proof.

Lemma 1. Given a convex n-gon W and n points P_k, one lying on each side of W. There is no nonzero vector $\boldsymbol{v}$ such that each $P_k + \boldsymbol{v}$ lies on an edge of W.

Proof. Assume $\boldsymbol{v}$ is such a vector and, by rotation of W to W^*, assume $\boldsymbol{v}$ is horizontal. Then if P_k is the point lying on one of the sides of W^* that contains the rightmost vertex of W^*, the $\boldsymbol{v}$-translation of P_k cannot lie on a side of W^*. ■

For the purpose of the rotor being fixed in space, we require contact with a sufficient number of sides such that those sides comprise an enclosing polygon. In the case of an odd-gon trammel, no two sides are parallel and the smaller arcs will make contact with two sides and thus all that is required is contact with at least one more side, which will form an enclosing triangle (necessarily convex); Lemma 1 then implies that the rotor cannot be translated in the plane and remain inside in the trammel.

So with reference to §2, we use the polygonal trammel to construct a sequence of triangles (the first is ΔABC in Fig. 5; note that ψ_1 is negative) and apply (3) to the problem of rotating each triangle around the two circles that start the rotor construction. In this way we determine the radii and centers of the circular arcs that make up the remainder of the rotor. In applying (3) it is important to recall the assumption that the two circles were equidistant from the x-axis. But in the case of the trammel the midpoint of the two circles is at $y_0 = (1 - \cos\alpha + r(1 - \sec\alpha))/2$; therefore when determining the centers of the circular arcs defining the envelopes an offset of y_0 needs to be added to the result. The values we need to

prescribe to use (3) are $\rho = r$ and $\delta = (1 + \cos\alpha - r(1 - \sec\alpha))/2$. The other parameters required are η, ψ_1, and ψ_2, all of which are specific to the polygon under consideration. Making these substitutions into (3) and now using E_y for the adjusted y-coordinate, we get the following formulas for the envelope:

$$E_x = (r(1 + \sec\alpha) - 1 - \cos\alpha)\cos\psi_1 \cos\psi_2 \csc\psi$$
$$E_y = \tfrac{1}{2}(1 + \cos\alpha - r(1 + \sec\alpha))\sin(\psi_1 - \psi_2)\csc\psi + y_0$$
$$E_{\text{rad}} = \eta - r(\cos\psi_1 + \cos\psi_2)\csc\psi$$

Note that all terms are linear in r, which means that as r runs from 0 to $\cos\alpha$ the radius E_{rad} varies linearly and further, the locus of the center E is a straight line. And we know that when $r = \cos\alpha$, then $E = (0, 0)$, the two circles defining the envelopes coalesce into one, and this circle is the incircle of the triangle defining the envelope. It follows that $E_{\text{rad}} = r = \cos\alpha$. Substitution of this result into the formula for E_{rad} enables us to derive the following formula: $\eta = (1 + (\cos\psi_1 + \cos\psi_2)\csc\psi)\cos\alpha$. This means that E_{rad} is given by $\cos\alpha + (\cos(\alpha) - r)(\cos\psi_1 + \cos\psi_2)\csc\psi$.

Thus all that remains to complete the general construction for an n-gon is to determine the values of ψ_1 and ψ_2. From geometrical considerations we know that the two sides in contact with the circles of the rotor form an angle of α, and so $\psi_1 + \psi_2 = \alpha$. Further, once we know the value of ψ_1 for one edge, the adjacent edge will have a value of ψ_1 that differs by 2α. From these considerations we learn that the ψ_i are given by

$$\psi_1 = \tfrac{1}{2}(4k - n)\alpha = 2k\alpha - \tfrac{\pi}{2} \text{ and } \psi_2 = \tfrac{1}{2}(n + 2 - 4k)\alpha = (1 - 2k)\alpha + \tfrac{\pi}{2} \tag{5}$$

where $1 \le k \le (n-1)/2$. The ψ_1 sequence is negative for the first half, and positive for the second half (and at the center if there is a center), while the ψ_2 sequence is simply the reverse of the ψ_1 sequence. And of course $\psi = \psi_1 + \psi_2 = \alpha$. Formulas (4) and (5) tell us that $\phi_{\min} = (1 - 2k)\alpha$ and $\phi_{\max} = \pi - 2k\alpha$.

Thus we have determined all the parameters necessary to define $(n-1)/2$ arcs on the right side of the rotor. We can now work around the polygon clockwise, using the envelopes to give a sequence of circular arcs, truncating each circle as it strikes the next and using symmetry—reflection in the y-axis—to handle the left side. Thus at the end we have a convex shape which will be the desired rotor; see Figure 6 where $n = 7$. We index the arcs clockwise starting from the first arc right of the upper auxiliary circle. In §4 we will prove that the circles intersect inside the polygon and that the rotor is stable within the trammel, meaning that its position is uniquely determined by its orientation.

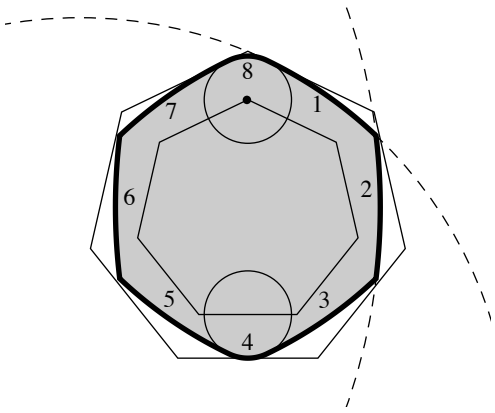

Figure 6. The circular envelopes intersect to form a rotor inside an n-gon. Here $n = 7$. The dashed circles show where arcs 1 and 2 intersect.

4. THE ARC INTERSECTIONS. To fully understand the rotor, both its definition and its stability within the trammel, we need to analyze the intersection points of each circular envelope arc with the next one (see Fig. 6). To this end we introduce two families of angles, $\phi_i(k, n, r)$, $i = 1, 2$ (we will suppress n and r, which are constant in any particular discussion). The definitions are based on the circles that define the arcs in Figure 6. Each such arc can be parametrized as $(X_k, Y_k) + R_k\,(\cos\phi, \sin\phi)$ where, in the notation of §2, (X_k, Y_k) would be $E_k = (E_x, E_y)$ and $R_k = E_{\text{rad}}$.

We introduce λ_k for the vector $E_{k+1} - E_k$ and ω_k for the angle made by this vector with the positive y-axis. Lemma 2 was discovered from the pictures: the centers E_k form a broken line with equal edges and equal angles (see Fig. 7, where $n = 11$). For the proof, we can use left-right symmetry and so restrict our investigation to k in $\{1, 2, \ldots, (n-1)/2\}$.

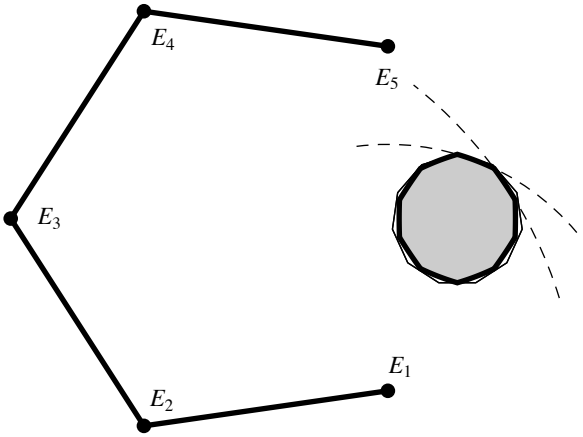

Figure 7. The centers of the circular envelopes lie on a path with equal lengths and angles.

Lemma 2. Assume $n \geq 3$ is odd and $1 \leq k \leq (n-1)/2$.

a. The length of λ_k is constant: $\|\lambda_k\| = 4\cos^2(\alpha/2)(\cos(\alpha) - r) = 2(1 + \cos\alpha)(\cos(\alpha) - r)$.

b. The angle made by λ_1 away from the negative y-axis is -5α.

c. The angles between successive λ_k all equal $\pi - 4\alpha$.

d. $\omega_k = (4k + 1)\alpha - \pi$.

Proof. Parts a–c are done using *Mathematica* to simplify the various algebraic and trigonometric expressions that arise. Part (d) follows from (b) and (c): using the supplementary angle to the successive angles, we get that the angle made by λ_k with the x-axis is $\left(\frac{3}{2}\pi - 5\alpha\right) - (k-1)(\pi - (\pi - 4\alpha)) = \frac{3\pi}{2} - (4k+1)\alpha$. But ω_k is measured from the y-axis, so $\omega_k = \frac{\pi}{2} - \left(\frac{3\pi}{2} - (4k+1)\alpha\right) = (4k + 1)\alpha - \pi$. ∎

Returning to the arcs, let $k = 1$ denote the first arc, with the arc-index increasing in clockwise order. We denote the intersection of the kth and $(k+1)$th arc by the values of the parametric variable ϕ. That is, the intersection point of arcs k and $k+1$ is given by $\phi_1(k)$ in terms of the kth circle and $\phi_2(k)$ in terms of the $(k+1)$st. To determine these angles we need to solve the equations

$$X_k + R_k\cos\phi_1(k) = X_{k+1} + R_{k+1}\cos\phi_2(k) \qquad Y_k + R_k\sin\phi_1(k) = Y_{k+1} + R_{k+1}\sin\phi_2(k)$$

By straightforward algebra:

$$R_{k+1}^2 = (X_{k+1} - X_k - R_k \cos\phi_1(k))^2 + (Y_{k+1} - Y_k - R_k \sin\phi_1(k))^2$$

Expanding the squares and rearranging yields

$$(X_{k+1} - X_k)\cos\phi_1(k) \; + \; (Y_{k+1} - Y_k)\sin\phi_1(k) \; = \; \frac{||\lambda_k||^2 + R_k^2 - R_{k+1}^2}{2\,R_k}$$

The angle ω_k satisfies $\sin\omega_k = \frac{X_{k+1}-X_k}{||\lambda_k||}$ and $\cos\omega_k = \frac{Y_{k+1}-Y_k}{||\lambda_k||}$; thus we may write $\sin\omega_k \cos\phi_1(k) + \cos\omega_k \sin\phi_1(k) = \frac{||\lambda_k||^2 + R_k^2 - R_{k+1}^2}{2\,R_k||\lambda_k||}$, or $\sin(\omega_k + \phi_1(k)) = \frac{||\lambda_k||^2 + R_k^2 - R_{k+1}^2}{2\,R_k||\lambda_k||}$.

There are of course two solutions in $[0, 2\pi]$; it turns out that the standard arcsine value yields a point on the part of the circle that forms the envelope, while the alternate value does not; so we use the standard arcsine.

Using Lemma 2a and d then gives:

$$\phi_1(k) = \arcsin\left(\frac{R_k^2 - R_{k+1}^2 + 16\,\cos^4\left(\frac{\alpha}{2}\right)(\cos(\alpha) - r)^2}{8\,R_k\,\cos^2\left(\frac{\alpha}{2}\right)(\cos(\alpha) - r)} \right) - (4\,k + 1)\,\alpha + \pi \tag{6}$$

Similarly we get

$$\phi_2(k) = \arcsin\left(\frac{R_k^2 - R_{k+1}^2 - 16\,\cos^4\left(\frac{\alpha}{2}\right)(\cos(\alpha) - r)^2}{8\,R_{k+1}\,\cos^2\left(\frac{\alpha}{2}\right)(\cos(\alpha) - r)} \right) - (4\,k + 1)\,\alpha + \pi$$

Note that $\phi_2(0)$ is just $(n-2)\,\alpha\,/\,2$.

We next prove that the construction leads to a convex shape, which we call the rotor.

Theorem 1a. Let $e_{1,k} = \frac{16\,\cos^4\left(\frac{\alpha}{2}\right)(\cos(\alpha) - r)^2 + R_k^2 - R_{k+1}^2}{8\,R_k\,\cos^2\left(\frac{\alpha}{2}\right)(\cos(\alpha) - r)}$, the argument to the arcsine in (6). Then $-1 \le e_{1,k} \le 1$. The same holds for $e_{2,k}$, the arcsine argument in ϕ_2.

b. The use of arcsine in (6) leads to points that lie on the envelope arcs.

c. The use of the alternate solution to the sine equation leads to points that do not lie on the envelopes.

d. When $n \le 99$ and $r = 0$, the intersection points of the envelopes lie on or inside the polygon.

Proof. a. We show that $e_{1,k}$ is increasing, and then verify that the extreme values are between -1 and 1. The lowest value corresponds to $k = 1$; for the upper we can invoke vertical symmetry to stop at $k = \lfloor (n-1)/4 \rfloor$. The proofs that $-1 \le e_{1,1}$, $e_{1,\lfloor (n-1)/4 \rfloor} \le 1$, and $e_{1,k} \le e_{1,k+1}$ when $1 \le k \le \lfloor (n-1)/4 \rfloor$ were carried out by computer algebra. The case of ϕ_2 is similar. The computer algebra here is nontrivial: we reduce the expressions to functions of $\cos\alpha$ and $\cos(k\,\alpha)$ and then call on *Mathematica*'s `Reduce` function, which uses cylindrical algebra decompositions to verify that the polynomials behave as claimed. For example, the smallest value, $e_{1,1}$, works out to

$$\frac{-\left((c-r)\left(c^2\,(4\,c+3) - (4\,c+1)\,s^2\right) + c\right)^2 + (c+1)^4\,(c-r)^2 + (r - 2\,c\,(c-r+1))^2}{4\,(c+1)\,(c-r)\,(r - 2\,c\,(c-r+1))^2}$$

where $c = \cos\alpha$, and this is what `Reduce` shows to be greater than -1.

b. We use the lower and upper bounds on the envelope-defining parameter ϕ given at the end of §3. It is routine to check that the lower bound is in $[-\pi, 0]$, while the upper is in $[0, \pi]$. Further, the value of ϕ_1 given in (5) lies in $[-\pi/2, 3\pi/2]$. So it suffices to show that ϕ_1 lies between the two bounds. But this too is routine, since replacing the arcsin in (5) by its extreme values $\pm\pi/2$ leads to very simple formulas. For example, $\phi_1 - \phi_{\min}$ is just $(n - 4 - 4k)\,\alpha/2$.

c. Next we show that the alternate sine-equation solution would be illegal as regards the envelope. Assume first that $e_{1,k} > 0$. Then the alternate value uses $\pi - \arcsin(e_{1,k})$ and will be larger. This case, and the others, are routine, because again the formulas simplify dramatically when $\pm\pi/2$ is used for the arcsine.

d. This is done by checking all j and k for each n and using *Mathematica*'s `Reduce` to verify that the points on the jth arc corresponding to legal values of ϕ are left of the kth polygon side (extended). ■

The evidence is overwhelming that the conclusion of part (d) holds in general, for all odd n and all values of r. The same is true for the stronger claim that any rotation of the rotor fits inside the polygon. For each rotation angle θ we can examine graphs to see that it is true, but a proof for all n and θ is lacking.

Conjecture. For any odd n and any r with $0 \le r < \cos\alpha$ the rotor as constructed here lies inside the polygon and, moreover, any rotation of the rotor can be translated so that it lies inside the polygon.

5. EXPLICIT CONSTRUCTION OF ROTORS. 5.1 The triangle For a triangle we have $n = 3$ and from (5), $\psi_1 = \psi_2 = \pi/6$. Thus after choosing some $r < 1/2$ we have the trammel with vertices at $(0, 1)$, $\left(\sqrt{3}/2, -1/2\right)$, and $\left(-\sqrt{3}/2, -1/2\right)$ and then two circles of radius r centered at $(0, 1 - 2r)$ and $\left(0, r - \frac{1}{2}\right)$, with the cutting tools of the rotor located at the centers of these circles. The rotor is completed with two arcs of radius $\frac{3}{2} - 2r$, centered at $\frac{1}{4}(1 - 2r)\left(-3\sqrt{3}, 1\right)$ and $\frac{1}{4}(1 - 2r)\left(3\sqrt{3}, 1\right)$. Two examples of such rotors are shown in Figure 8, with r being 0 and 0.2. Note that both in proofs and when writing code for animations we can use symmetry: the situation at the end of the rotation interval $0 \le \theta \le \pi/n$ is just a rotation of the initial state.

An animation of the motion in this case, and all odd-n cases, is available at [**CW2**]. When $r = 0$ we have stability because of the third point of contact that arises from the envelope construction. Note that the other two points of contact, at the cusps, both serve as cutting points, and so they work together to trace out the final triangle; the progress is indicated in Figure 8 by the bold lines showing the locus. In the image at right the auxiliary radius is 0.2 and the rotor is made up of four arcs; the tangency giving stability works in the same way as in the $r = 0$ case. The case of the rotating lens ($r = 0$) was first discovered by F. Reuleaux [**R**, chap. III], though in the context of rotational mechanics as opposed to polygonal drills.

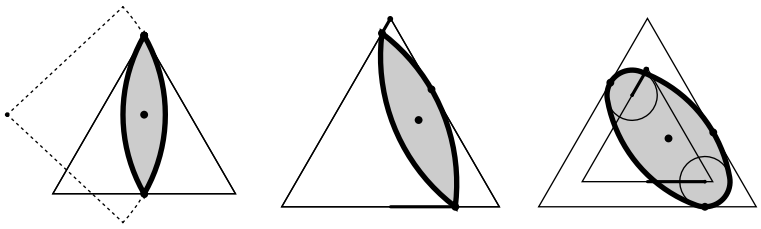

Figure 8. The rotor for a triangle. At left and center the auxiliary circles vanish ($r = 0$) so the rotor consists of just two circular arcs. The central image shows how stability arises from the tangent point at right. At far right $r = 0.2$ and the rotor is bounded by four circular arcs.

5.2 The pentagon and the *vesica pisces* For the pentagon, n is 5 and there are two different values for each of ψ_1 and ψ_2 as k can be 1 or 2. The first arc is constructed using $\psi_1 = -\pi/10$ and $\psi_2 = 3\pi/10$ while the second uses $\psi_1 = -\pi/10$ and $\psi_2 = 3\pi/10$. As always the trammel has reflective symmetry and therefore the arcs on the left side are just reflections of the arcs on the right. Two examples of such constructions are in Figure 9: $r = 0$ and $r = 0.4$. The first case presents a surprise: the rotor is exactly the intersection of two shapes known as *vesica pisces* (fish bladder). This shape, the intersection of two circles of the same radius arranged so that the center of each is on the other, appears often in geometrical art, and two copies of the shape appear, truncated, in Figure 9 (oriented horizontally, the leftmost with a dashed border, the other with solid border). Their intersection is the rotor.

For $r > 0$ the situation is shown at center and right in Figure 9; stability holds because the upper right tangent point maintains tangency beyond the point at which the lower-right arc attains tangency (proof in §5.3). In the rightmost image the tangent point at upper right is about to disappear, but the one on the lower right has been rolling on the trammel for a while, so at all times we have the three points we need for stability.

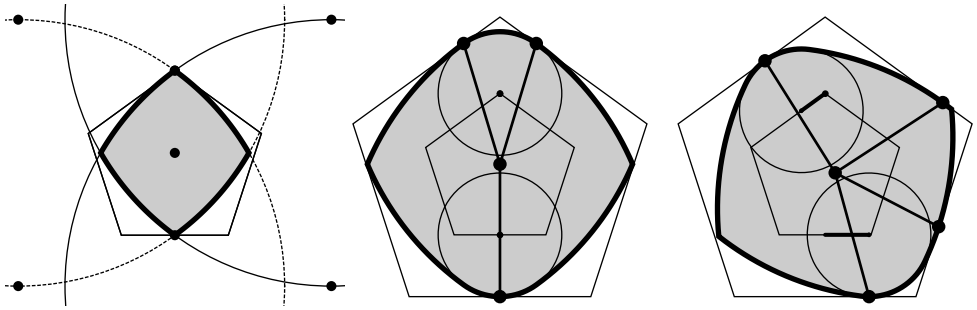

Figure 9. The rotor for a pentagon. At left there are no auxiliary circles and the rotor is the intersection of two vesica pisces shapes. In the rightmost two images $r = 0.4$; stability arises from the fact that the tangent point at lower right in the rightmost image shows up before the one at upper right disappears.

5.3 More sides: proof of stability The case of a 9-gon is shown in Figure 10, with frames illustrating one complete period ($0 \le \theta \le \pi/n$). Ten circular arcs define the rotor. Tangencies are marked with radial lines. It was not until we animated the process that we learned the useful fact—the miracle alluded to in §3—that the lower-right tangency (arising in the fifth frame of the figure) arises before the upper-right

one disappears. This phenomenon gives stability without the need to worry about the arrival time of any of the other tangency points (the ends of the dashed lines).

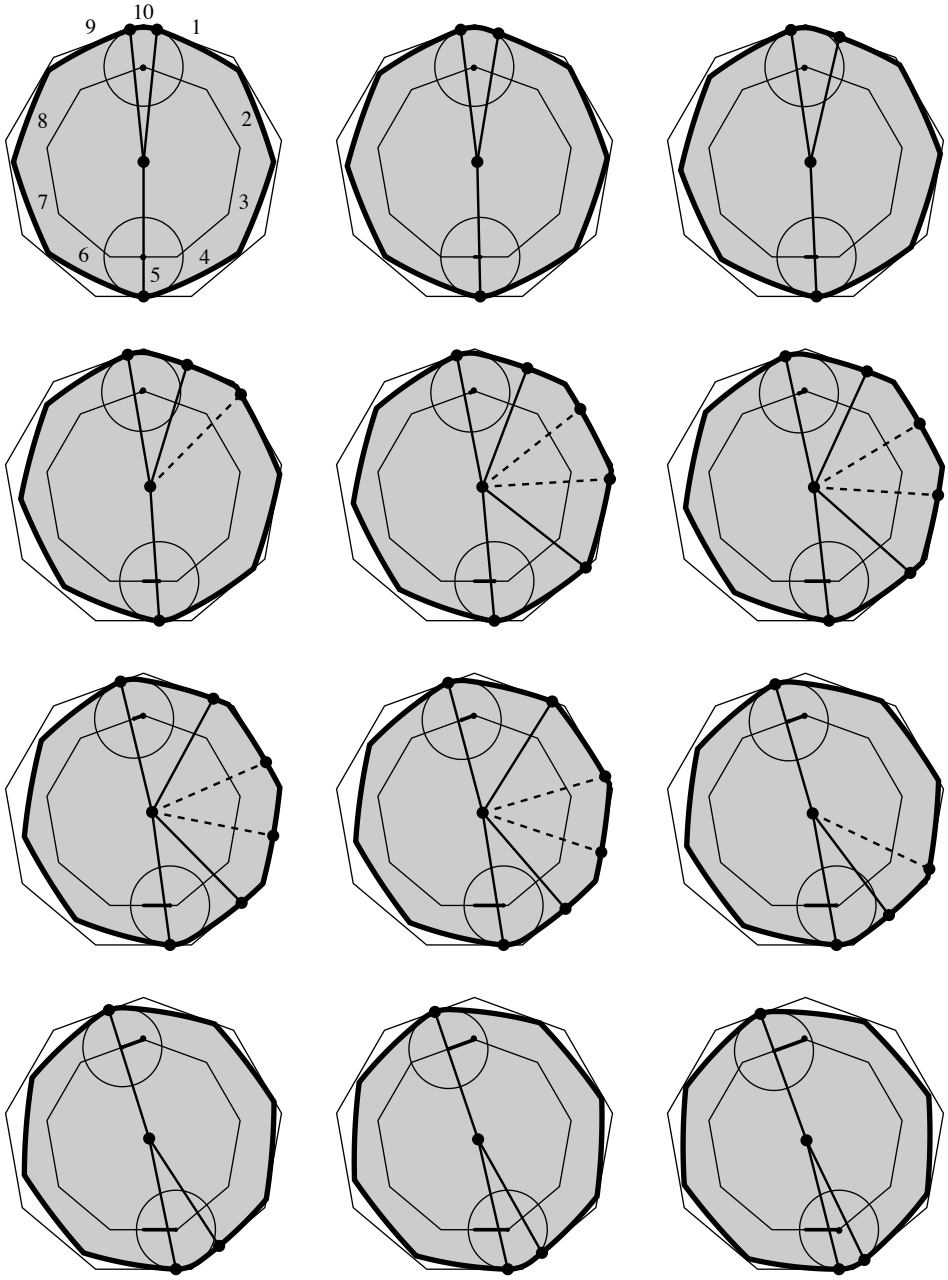

Figure 10. The images correspond to equal amounts of rotation as θ runs from 0 to $\pi/9$—one period—for the $n = 9$ case. The final step ($\theta = \pi/9$) is just a rotation by $10\pi/9$ of the initial state. Stability comes from tangent points attached to solid lines. In the first eight frames the one at upper right is sufficient; in the last eight we have the one at lower right. The overlap of these frames gives stability throughout, without having to rely on the intermediate tangent points (the dashed radial lines).

If we index the boundary arcs as in the first frame of Figure 10, then the assertion that the tangency of arc 1 overlaps (in terms of the rotation) with the interval for which arc number $(n-1)/2$ (arc 4 in the

figure) is tangent to the trammel is equivalent to the inequality $(n-3)\,\alpha \geq 2\,\phi_1(1, n)$, where $\alpha = \pi/n$ and ϕ_1 was defined in §4.

Lemma 3. For $n \geq 5$ and odd, the overlap of the tangency of arcs 1 and $(n-1)/2$ is equivalent to the inequality $\pi - 3\,\alpha \geq 2\,\phi_1(1, n)$.

Proof. In the initial state (Fig. 10, first frame), arc 1 is tangent to its corresponding side, and the tangent point corresponds to $\theta = (n-2)\,\alpha/2$ in the parametrization of the envelope-circle. This is because $\theta = 0$ in the parametrization corresponds to the envelope-defining line being vertical (see §2), while here we are $\frac{\pi}{2} - \alpha$ away from vertical. The tangency holds until the envelope-circle parameter reaches $\phi_1(1)$. Therefore the amount of rotation, starting from the initial state, during which arc 1 is tangent is $(n-2)\,\alpha/2 - \phi_1(1)$.

To reach the end of the first period (last frame in Fig. 10) the amount of rotation is α. The first tangency of arc number $(n-1)/2$ occurs before this and by symmetry the amount of rotation for which the tangency exists is the same quantity as for arc number 1: $(n-2)\,\alpha/2 - \phi_1(1)$. Thus the claimed overlap occurs provided $(n-2)\,\alpha/2 - \phi_1(1) \geq \alpha - ((n-2)\,\alpha/2 - \phi_1(1))$, which is equivalent to the claimed inequality. ∎

The inequality of the lemma is true; we will prove it with the help of *Mathematica* to simplify complicated trig expressions. Note that the inequality can, in some cases, just barely hold: if $n = 17$ and $r = 0$ then the duration of joint tenure—the amount of rotation for which the two tangencies hold—is under 1°.

Theorem 2. For $n \geq 5$, $\pi - 3\,\alpha > 2\,\phi_1(1, n)$, where $\alpha = \pi/n$.

Proof. We start with formula (6) for ϕ_1; using the *Mathematica* functions `Simplify` and `TrigExpand` the inequality gets transformed to

$$7\,\frac{\alpha}{2} - \frac{\pi}{2} + \arcsin\left(\frac{2\,r - 1 - 2\,(1-r)\cos\alpha + \cos(2\,\alpha) + (2 - 4\,r)\cos(3\,\alpha) + 3\cos(4\,\alpha) - 2\,r\cos(5\,\alpha) + \cos(6\,\alpha)}{2\,(1 - r + 2\,(1-r)\cos\alpha + \cos(2\,\alpha))}\right) > 0$$

Isolating the arcsin, applying sine to both sides, and simplifying transforms this to:

$$\cos\left(\frac{7\,\alpha}{2}\right) < \frac{1 - 2\,r - 2\,(1-r)\cos\alpha - \cos(2\,\alpha) - (2 - 4\,r)\cos(3\,\alpha) - 3\cos(4\,\alpha) + 2\,r\cos(5\,\alpha) - \cos(6\,\alpha)}{2\,(1 - r + 2\,(1-r)\cos\alpha + \cos(2\,\alpha))}$$

Then replacing α by $2\,\beta$, expanding the cosines, and using c for $\cos\beta$ yields an inequality that is just a quotient of terms that are linear in r:

$$\frac{p(c) + q(c)\,r}{4\,c^2\left(2\,c^2 - 1\right) + \left(1 - 4\,c^2\right)r} < 0 \tag{7}$$

where $p(c) = 4\,c^2(1-c)\left(1 - 2\,c^2\right)\left(17 + 24\,c - 96\,c^2 - 152\,c^3 + 144\,c^4 + 256\,c^5 - 64\,c^6 - 128\,c^7\right)$
and $q(c) = (1-c)\left(4\,c^2 - 1\right)\left(5 + 12\,c - 56\,c^2 - 112\,c^3 + 112\,c^4 + 224\,c^5 - 64\,c^6 - 128\,c^7\right)$.

Inequality (7) can be proved by using the conditions $0 \leq r < \cos\alpha = 2\,c^2 - 1$ and $0.95 < \cos(\pi/10) \leq \cos\beta = c < 1$. These conditions easily imply that the denominator in (7) is positive. For the numerator, p and q vanish at $c = 1$, have positive derivative at $c = 1$, and have no roots in $(0.9, 1)$; hence they are both negative when $0.95 < c < 1$ and $r \geq 0$; the entire numerator is therefore negative. ∎

The following corollary implicitly assumes the truth of the Conjecture in §4.

Corollary. For every regular polygon with an odd number of sides, the rotor as constructed here is stable within the trammel; that is, for every orientation there is a unique position of the rotor inside the trammel.

Proof. By Lemma 3, Theorem 2, and the discussion in §5.1 for the triangle. ■

The outstanding open problem in this area is to find a uniform method for a rotor that has a point tracing a perfect n-gon when n is even and beyond 8. But in the odd case, even though computational experiments leave little doubt that our construction is sound, there remains the problem of finding rigorous proofs that the rotor is well-defined and fits inside the trammel in all orientations and for all values of n and r.

REFERENCES

[BS] J. Bryant and C. Sangwin, *How Round Is Your Circle?,* Princeton University Press, Princeton, N.J., 2008; associated website: http://HowRound.com (enter site and click on Applications of Non-Roundness).

[CW] B. Cox and S. Wagon, Mechanical circle-squaring, *College Mathematics Journal,* **40** (2009) 238–247.

[CW1] B. Cox and S. Wagon, Drilling a hexagonal hole, The Wolfram Demonstrations Project, available at http://demonstrations.wolfram.com/DrillingAHexagonalHole.

[CW2] B. Cox and S. Wagon, Drilling an n-gon hole for odd n, The Wolfram Demonstrations Project, available at http://demonstrations.wolfram.com/DrillingAnNGonHoleForOddN.

[G] M. Gardner, *Further Mathematical Diversions*, Penguin, New York, 1969, 212–215.

[G1] M. Goldberg, Circular-arc rotors in regular polygons, American *Mathematical* Monthly **55** (1948) 393–402.

[K] S. Kabai, Oldham coupling, The Wolfram Demonstrations Project, available at http://demonstrations.wolfram.com/OldhamCoupling.

[R] F. Reuleaux, *The Kinematics of Machinery*, Macmillan, London, 1876.

[W] S. Wagon, Drilling a square hole, The Wolfram Demonstrations Project, available at http://demonstrations.wolfram.com/DrillingASquareHole.

[W1] S. Wagon, Square hole drill in three dimensions, The Wolfram Demonstrations Project, available at http://demonstrations.wolfram.com/SquareHoleDrillInThreeDimensions.

BARRY COX, University of Adelaide, SA 5005, Australia
barry.cox@adelaide.edu.au

STAN WAGON, Macalester College, St. Paul, Minnesota 55105, USA
wagon@macalester.edu